16.3 COMPARISON OF CLOUD-RESOLVING ENSEMBLE SIMULATIONS USING LM AND MC2 SIMULATIONS

Cathy Hohenegger[(1)]*, Christoph Schär[(1)], André Walser[(2)] and Daniel Lüthi[(1)]

[1]Institute for Atmospheric and Climate Science, ETH, Zürich, Switzerland

[2]MeteoSwiss, Zürich, Switzerland

1. INTRODUCTION

The use of imperfect numerical weather prediction models combined with the chaotic nature of the atmospheric dynamics strongly limits weather forecasting capabilities. In a previous study by Walser and Schär (2004), the different levels of predictability between the two MAP cases IOP2b (19-20.09.1999) and IOP3 (24-25.09.1999) were demonstrated using cloud-resolving MC2 ensemble simulations. The same cases are here investigated by means of simulations performed with the Lokal Model LM. The comparison of both ensembles aims to better isolate predictability limitations arising from the chaotic nature of the atmosphere upon which some hypotheses regarding the different predictability levels in IOP2b and IOP3 may be formulated.

Both ensembles are constituted of six members initialized with one hour time lag: the first member starts at 16h00 on the 19th (24th) September, the second one at 17h00 and so on until 21h00. Their boundary data depend on the model-chain. For MC2, two simulations are performed: the first one with the CHRM model on a 0.125° by 0.125° grid using ECMWF operational analysis as boundary data and the second one with the MC2 model runned at 14km whose output serves to drive the high-resolution ensemble simulations at 3km. For the LM, the ECMWF operational analysis drives a first LM simulation at 7 km which is then used to integrate the different ensemble members at 2km resolution. This approach uses identical lateral boundary conditions for the six members of each ensemble and thus assumes perfect predictability on the synoptic scale. This is useful to focus on small-scale error growth in the interior of the computational domains. The obtained results are illustrated in the next section.

2. RESULTS

2.1 Precipitation

The daily accumulated precipitation obtained by averaging the six members of the MC2 and of the LM ensemble is illustrated on Figure 1 for IOP2b and for IOP3. Both models succeed in representing the strong precipitation event associated with IOP2b over the southern Alpine region and the occurrence of south-westerly elongated precipitation bands over the Jura and Ticino regions in IOP3. The overall precipitation intensity, the position of maxima and the small-scale features show nevertheless stronger discrepancies. Compared to MC2, the LM model especially misses rain in the lee of the Alps while simulating larger amounts elsewhere.

The differences observed in the precipitation pattern on Figure 1 can be attributed to a combination of two factors. First, both models use different physical parameterizations, each of them being of imperfect nature. Their well-known drawbacks, i.e. underestimation of precipitation by about 40% in the MC2 model (see Benoit et al. 2002), overestimation of rain over mountain peaks and corresponding underestimation in their lee in the LM model (see Steppeler et al. 2003) can clearly be recognized in Figure 1. The use of a steeper topography in the LM model further accentuates this behavior. Secondly, the model-chains and the extent of the integration domains are not fully identical. The larger extent of the LM domain on its western side particularly contributes to the simulated differences in typical south-westerly situations as in IOP3.

2.2 Spread evolution

Figure 2 shows time series of the normalized standard deviation of precipitation on the 20th and 25th September as averaged over Ticino and Jura together with the simulated mean precipitation. In terms of the amplitude of the spread, it should be here noted that in this study we are using small-amplitude initial errors (see Walser et al. 2004 for further discussion). Despite varying precipitation amounts (as already seen on Figure 1), the MC2 and LM ensembles show a surprising level of agreement in the evolution of their spread. This is particularly the case over the Ticino area and

**Corresponding author:* Cathy Hohenegger, Institute for Atmospheric and Climate Science ETH, Winterthurerstrasse 190, 8057 Zurich, Switzerland. Email: cathy.hohenegger@env.ethz.ch

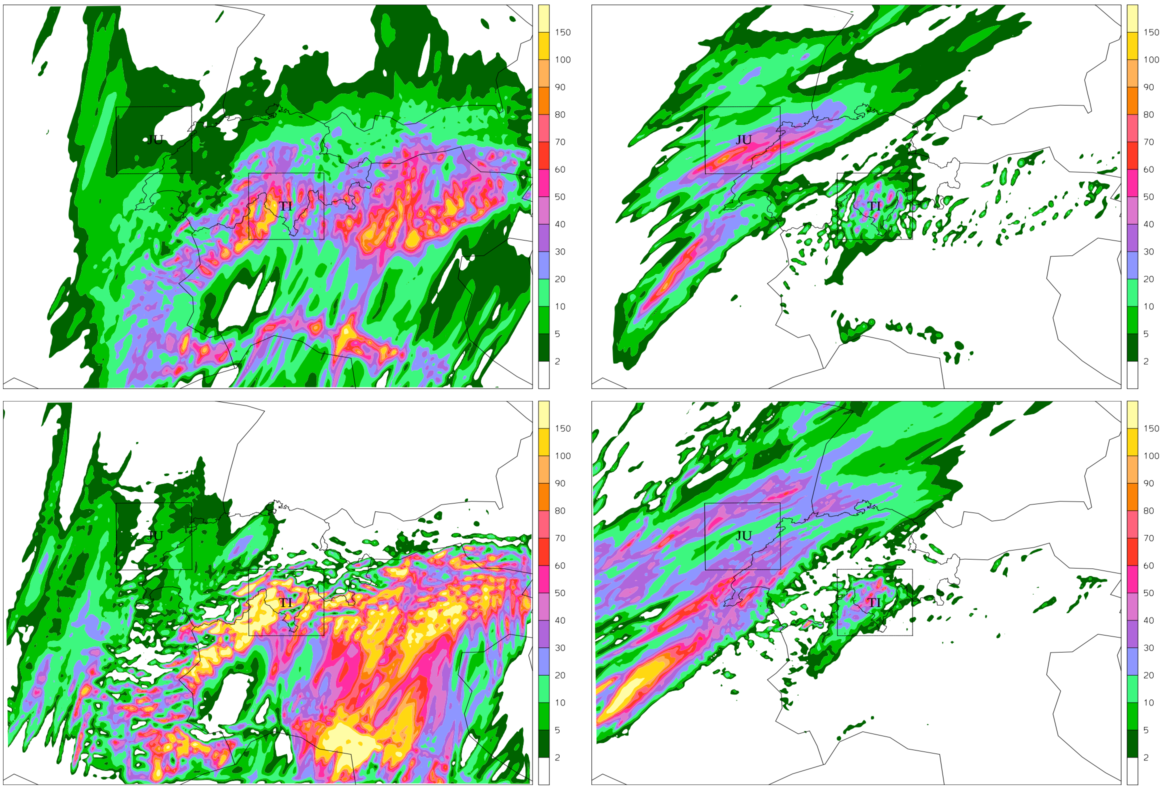

Figure 1: Daily accumulated precipitation (mm) on the 20th of September 1999 (IOP2b, left) and on the 25th of September 1999 (IOP3, right) obtained by averaging the six MC2 (top) and LM (bottom) ensemble members.

correlates well with the similar precipitation behavior observed in both models. Correspondingly, the partial disagreement in the evolution of mean simulated precipitation between MC2 and LM, as apparent over Jura on the 25th September, can be tracked back to the time series of their standard deviation. It may be concluded that, independently from the simulated precipitation amount, the spread obtained through different model setups remains comparable as long as the precipitation evolution behaves similarly in each ensemble (i.e. as long as we can assume perfect predictability on the synoptic scale). Since such a behavior could also be observed with other climate elements (e.g. temperature), the flow evolution mainly determines the associated error growth in IOP2b and IOP3.

Figure 2 also pinpoints IOP3 as the case with lower predictability than IOP2b, independently of the chosen model formulation. The use of a normalized spread may bias this interpretation since IOP2b is generally associated with stronger precipitation intensity than IOP3. Moreover, differences can only be seen when it is raining. It may be more appropriate to say that IOP3 generally sustains the development of stronger, larger-scale and longer-lasting perturbations than IOP2b, as further illustrated in the next section.

2.3 Reasons for the different predictability levels

The distinct levels of predictability in IOP2b and IOP3 can be attributed to the different flow evolutions between both cases. This is best visible when introducing a small perturbation at initial time (e.g. in the temperature field) and following its development through the forecasting period. Since the most active precipitation phase occurs in IOP2b in the morning compared to the late afternoon in IOP3, we consider here the differences obtained at 9h00 on the 20th of September and at 17h00 on the 25th, as illustrated on Figure 3. Figure 3 shows the response of the temperature field in the lowest LM model layer to the introduced perturbation. A perturbation visible in the temperature field will also lead a signature in precipitation if raining. Both cases sustain the development of temperature differences, which are of a much more localized and weaker nature in IOP2b than in IOP3. Moreover, the southern Alpine region experiencing in IOP2b the frontal passage with its associated precipitation remains mostly unperturbed in opposition to its counterpart (western side of the Jura chain) in IOP3 (compare pan-

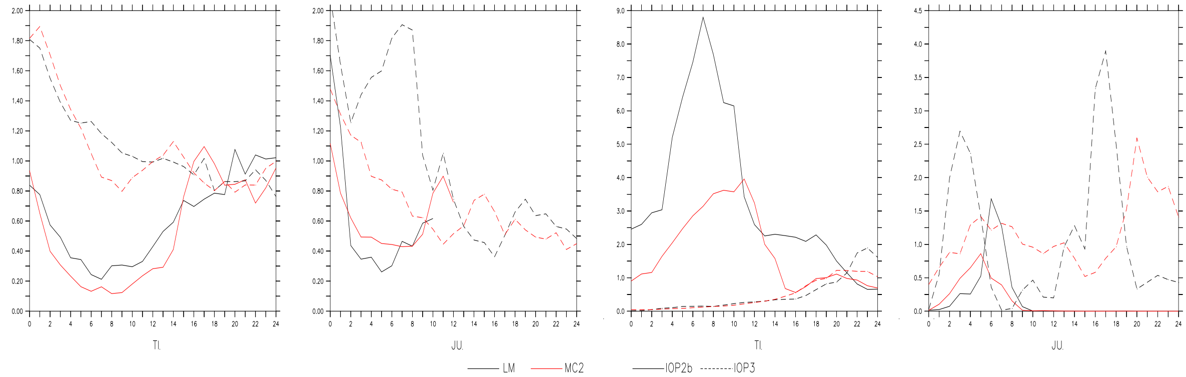

Figure 2: Time series of the normalized standard deviation of precipitation (left plots) together with the mean simulated precipitation (right plots) averaged over Ticino (TI) and Jura (JU) for IOP2b (20.09.1999) and IOP3 (25.09.1999) in mm/h. The location of the Ticino and Jura regions can be found on Figure 1.

els in Figure 3). The upscaling contamination of the mesoscale flow by local instabilities growing over convective regions, as shown in Zhang et al. (2003), seems to be sustained in IOP3 but not in IOP2b, and may thus explain their different levels of predictability.

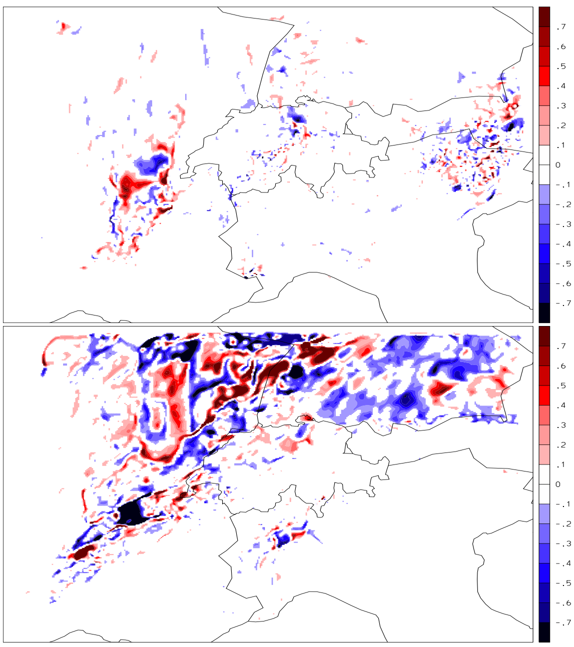

Figure 3: Difference obtained in the temperature field in the lowest LM model layer when slightly perturbing an ensemble member, i.e. a bell-shape localized perturbation was introduced in the initial temperature distribution of the LM member starting at 21h00. The time is 9h00 on the 20th September for the uppper plot and 17h00 on the 25th September for the lower one.

3. CONCLUSION

A comparison of cloud-resolving ensemble simulations integrated with the MC2 and LM models was performed. Despite characteristic differences in their simulated precipitation field, which may be mainly related to limitations in model formulation and parameterization packages, they associate similar synoptic situations with similar levels of predictability. Hence, by assuming perfect predictability on the synoptic scale, the flow evolution mainly determines small-scale error growth in the computational domain and the predictability levels associated with distinct MAP cases.

REFERENCES

Benoit, R. and Coauthors, 2002: The real-time ultrafinescale forecast support during the special observing period of the MAP. *Bull. Amer. Meteor. Soc.*, **83**, 85–109.

Steppeler, J. and Coauthors, 2003: Meso-gamma scale forecasts using the nonhydrostatic model LM. *Meteorol. Atmos. Phys.*, **82**, 75–96.

Walser, A., D. Lüthi, and C. Schär, 2004: Predictability of Precipitation in a Cloud-Resolving Model. *Mon. Wea. Rev.*, **132**, 560–577.

Walser, A. and C. Schär, 2004: Convection-resolving precipitation forecasting and its predictability in Alpine river catchments. *J. Hydrol.*, **288**, 57–73.

Zhang, F., C. Snyder, and R. Rotunno, 2003: Effects of Moist Convection on Mesoscale Predictability. *J. Atmos. Sci.*, **60**, 1173–1185.